Q19990617 0003

Stochastic Analysis of Early Tracer Arrival in a Multiple-Fracture Pathway

Scott Painter
Center for Nuclear Waste Regulatory Analyses, Southwest Research Institute
San Antonio, Texas

Vladimir Cvetkovic
Division of Water Resources Engineering, Royal Institute of Technology
Stockholm, Sweden

Short title: MULTIPLE-FRACTURE PATHWAY

Abstract. A stochastic model for transport and retention in fractured rock is proposed as an alternative to more elaborate numerical simulations. Contaminants are transported by advection through a series of n rock fractures. The microscopic processes of matrix diffusion and sorption act together to retain contaminants in the host rock. The transport pathway is characterized by large-scale fluctuations in the advection velocity caused by spatial variability in the fracture attributes along the pathway. The moments of the time-of-arrival of an initial solute pulse are related in a generic way to the joint distribution of fracture aperture and length. These moments are controlled primarily by a dimensionless retention parameter that incorporates all the deterministic model parameters and by correlation between fracture length and aperture. The results show that a systematic bias in the predicted contaminant transport can be introduced by neglecting spatial variability in fracture attributes. The relative contributions of fracture-to-fracture variability and within-fracture variability are also explored. The proposed stochastic methodology can incorporate empirical data directly or can be merged with relatively simple numerical simulations to broaden the applicability.

Introduction

Geological isolation of radioactive waste relies on stable, low-permeability rock as an important barrier to the release of radionuclides to the biosphere. Transport in these low-permeability rock barriers occurs mainly by advection through interconnected networks of fractures but is slowed by microscopic processes that act to retain particles in the surrounding rock. As particles are swept along by water flowing in the rock fractures, they can diffuse into the stagnant (or relatively slowly moving) water in the pore space of surrounding rocks where they may sorb onto mineral grains. These microscopic retention mechanisms act together to retard the downstream movement in a nonlinear fashion. As part of ongoing safety assessments of proposed waste isolation facilities, it is necessary to have quantitative predictions for the time required for radionuclides to migrate through the rock barriers, taking into account advection and retention processes.

Transport in fractured rock is further complicated by uncertainty in the transport pathways, as it is usually not possible to have direct observations of subsurface features. The best that could be hoped for in a typical application is to know the statistics of fracture attributes, such as aperture and length. This uncertainty requires that radionuclide migration, and the related issue of waste repository performance assessment, be addressed in a probabilistic framework. In a previous paper [*Painter et al.*, 1998], we outlined in general terms such a framework, taking into account advective transport through a series of connected fractures combined with matrix diffusion and sorption in the host rock. In this paper, we develop the methodology further, focusing on the arrival time t_ϕ of a specified mass fraction ϕ. This fractional arrival time is a useful measure of the effectiveness of the natural barrier. Of particular interest is t_ϕ for early arrivals (e.g. $\phi = 1\%$ or 5%), which represents the leading edge of the plume.

Most modeling studies of transport in fractured rock use continuum models in which the network of rock fractures is replaced by an equivalent porous medium. In

such models, retention in the rock matrix is accounted for by defining two interacting continua, one for the fractures and a second for the rock matrix. The rock matrix is modeled as either a second flow system [*Pruess and Narasimhan*, 1985; *Berkowitz et al.*, 1988; *Birkholzer et al.*, 1993] or as a nonflowing reservoir accessible through diffusive mass exchange [*Foster*, 1975; *Grisak and Pickens*, 1980; *Neretnieks*, 1980; *Bibby*, 1981]. Prediction uncertainty can be addressed in continuum models by making the effective medium properties a random space function. In this stochastic-continuum approach, geostatistical methods can be used to generate effective properties in unobserved regions.

Continuum models are appropriate when the fracture density is much greater than the threshold for percolation and the scale-of-support for the continuum-level properties is much larger than the largest fractures. Discrete-fracture models provide alternatives when these two conditions are not met. The discrete-fracture approach is based on networks of idealized fracture elements in two [*Long et al.*, 1982; *Schwartz et al.*, 1983; *Smith and Schwartz*, 1984] or three spatial dimensions [*Long et al.*, 1985; *Shapiro and Andersson*, 1985; *Andersson and Dverstorp*, 1987; *Cacas et al.*, 1990]. More realistic models also take into account spatial variability within the individual fractures [*Nordqvist et al.*, 1992] or mass exchange with the host rock [*Moreno and Neretnieks*, 1993; *Kupper et al.*, 1995; *Barten*, 1996].

Our approach is of the discrete-fracture variety but avoids the Monte Carlo fracture network simulation characteristic of that approach. Instead, we derive moments of the flux and related quantities analytically. This approach is made possible by a simplifying assumption, justified by field observations and previous network simulations, which allows us to replace a complex interconnected fracture network with an idealized migration pathway formed by n fractures connected in series. Specifically, we neglect dispersion caused by fracture intersections and also within single fractures and focus on the dominant pathway through the network. Transport and mass exchange within this transport pathway are modeled in a manner similar to Cvetkovic *et al.* [1999]

who applied the Lagrangian framework for transport in aquifers [*Cvetkovic and Dagan*, 1994, 1996; *Dagan and Cvetkovic*, 1996] to single fractures with variable aperture. The focus here is on a transport pathway consisting of *multiple* fractures and characterized by large-scale fluctuations in the advective velocity.

The approach taken here has some similarities to that of Moreno and Neretneiks [1993]. They conceptualize the transport as occurring in a cubic network of randomly varying "channels" and use an approach similar to ours for the transport in each channel. Nevertheless, the two approaches are fundamentally different in that we employ a new conceptual model appropriate for the limiting situation of negligible dispersion. This approach allows prediction uncertainty to be addressed analytically instead of through Monte Carlo simulations.

Conceptual model of a migration pathway

We consider water flowing through a three-dimensional fractured medium. The flow takes place predominantly through conductive fractures. If the entire geometry of the system was specified and all the relevant parameters known, the flow field could, in principle, be solved for given boundary conditions. The result would yield the water velocity field, $\mathbf{v}(\mathbf{x})$, applicable at a given scale. In practice, the required information is not available and we employ various approximations and a stochastic framework to solve the flow and transport problem.

We consider tracers released into a fracture over a small area ΔA_0 located at $\mathbf{x}_0$. Water flows through the release area ΔA_0 with constant volumetric rate Q [$\mathrm{L}^3\mathrm{T}^{-1}$]. The cross-sectional area ΔA_0 defines the "streamtube" (or a flowpath) from the source point to a specified "compliance boundary" located downstream from $\mathbf{x}_0$ along the mean flow direction. An example would be an injection point $\mathbf{x}_0$ from a single failed canister in a repository, with the biosphere as the compliance boundary. Note that the scale of the cross-sectional area ΔA_0 defines the relevant scale of the flow problem. In the

general case, the injected tracer is advected by the velocity $\mathbf{v}$, is dispersed by small-scale fluctuations, and is subject to mass transfer reactions such as sorption and/or diffusion into the immobile water of the rock matrix.

Flow and advective transport

We make the following simplifying assumptions regarding flow and advective transport:

- Advection along an indivisible streamtube is the dominant physical transport mechanism; dispersion within fractures is neglected, as is branching of the streamtube at fracture intersections.
- The tracer is advected by a constant water volumetric flow rate Q.
- The streamtube/flowpath for the advecting solute is through intersecting fractures, whereby flowpath segments are planar fractures with variable aperture $b(\mathbf{x})$; a sequence of n connected fractures forms a transport pathway through an otherwise impermeable medium (Figure 1).
- The cross-sectional area of the streamtube/flowpath at any given point is rectangular, with $b(\mathbf{x}) \ll w(\mathbf{x})$, where $w(\mathbf{x})$ is the width of the streamtube at $\mathbf{x}$.

The neglect of dispersion within individual fractures is appropriate in the present context, since our focus is on global quantities such as the arrival time at a receptor group. Global quantities are known to be little affected by local dispersion [*Dagan*, 1989], in contrast to spatial moments of local quantities such as solute concentration, which can be sensitive to local dispersion (e. g., Dagan and Fiori [1997]).

Our main simplification is to neglect downstream branching in the flowpath. In the general situation, networks of interconnected fractures contain multiple paths for tracers to traverse the network. This multiply-connected nature of networks is the principal

barrier to analysis in the general situation, and the reason previous transport modeling studies relied heavily on Monte Carlo network simulations. We do not attempt to model the most general situation, but focus instead on a limiting situation with practical and theoretical significance. Specifically, we ignore multiple pathways through the network and consider networks characterized by a dominant pathway for tracer migration.

This focus on a single dominant transport pathway is consistent with a barely connected network near the percolation threshold. More importantly, it is supported by numerical and field evidence. Monte Carlo network simulations using field-derived fracture attribute distributions reveal that a small number of transport pathways is often responsible for the majority of the mass flux [*Dverstorp et al.*, 1992], particularly when the particle source is spatially localized. Such large-scale channelization of flow and transport is observed frequently in field experiments [*Neretnieks*, 1993].

Besides being supported by numerical and field evidence, the neglect of downstream branching in the transport pathway is also of interest as a limiting situation that provides a conservative bound for the effect of interest in many applications. When viewed at the macroscopic scale, downstream bifurcations in the flowpath act to spread the migrating contaminants in both longitudinal and transverse directions. This macroscopic dispersion acts to dilute the migrating plume. Thus, our simplifying assumption about the flowpath will lead to an underestimate of the dilution and an overestimate of peak dose at a receptor group or the compliance boundary.

Streamtube characterization

The streamtube, or flowpath, is determined by two streamlines bounding the initial release, and its width is set by the width w_0 of the initial release. If the aperture at the release point is $b(\mathbf{x}_0)$, then the source cross-sectional area is $\Delta A_0 = b_0\, w_0$. Fluid passes through the streamtube at a constant flowrate, Q, and the magnitute of the initial velocity is $|\mathbf{v}(\mathbf{x}_0)| = Q/b_0\, w_0$.

Local variations in the fracture aperture will cause the streamtube width to fluctuate about w_0. Aperture variations will also cause the flowpath trajectory to meander through the individual fractures. This meandering is irrelevant in the present context. The relevant cross-sectional area for the streamtube is the one orthogonal to the mean flow direction, as this determines the fluid residence time. We thus define a kinematic prototype of a flowpath in one dimension, with varying aperture $b(x)$ and width $w(x)$ where x is the distance *along* the flowpath trajectory (i.e., an intrinsic coordinate).

We use a shifting-mean model to generalize this model to a multiple-fracture situation (Figure 2). Here the local spatial average aperture is piecewise constant. It undergoes stepwise changes as the flowpath passes from fracture to fracture. The notation introduced in Figure 2 is as follows: $b_i(x_i)$ is the fracture aperture in the i-th segment, $w_i(x_i)$ is the fracture width, x_i is the distance along the trajectory starting at the beginning of the i-th segment, $\bar{b}_i$ is the spatially averaged aperture of the i-th segment, and l_i is the length of the i-th segment.

If the fracture attributes, length l_i and aperture $b_i(x_i)$, are known for each segment in the chain, the time-dependent solute concentration or flux at the output of the n-th fracture could be calculated deterministically. In practice, however, the fracture lengths and apertures are known only statistically. That is to say, the fracture attributes are unobserved but have a specified joint probability density function that can be estimated from site characterization studies. In this case, the solute flux and related quantities become probabilistic quantities, which we relate to the random variables describing $\bar{b}_i$ and l_i.

The local fluctuations around the mean values w_0 and $\bar{b}_i$ are an additional source of prediction uncertainty. This uncertainty can be addressed by making $w_i(x_i)$ and $b_i(x_i)$ random space functions (RSF). Although internal variability within a single fracture is clearly important in some situations, fracture-to-fracture variability is often much

larger and is expected to dominate. Therefore, we concentrate on the situation with no internal variability and set $b_i(x_i) = \bar{b}_i$ and $w_i(x) = w_0$. However we return to the more general situation in section 8 and demonstrate how the internal variability can be included in the analysis.

Mass transfer processes

The downstream movement of the solutes is slowed by matrix diffusion, the process by which the solute diffuses into and out of the stagnant fluid in the pore space of the surrounding medium, and by equilibrium sorption on the contact surfaces.

We consider *diffusion into the rock matrix*, *sorption in the matrix*, and *sorption on the fracture surfaces* as key mass transfer reactions in a fractured formation. To formulate and solve the transport problem, we adopt the following simplifying assumptions:

- All mass transfer reactions are linear.
- The movement of tracers in the rock matrix is assumed to be due to molecular diffusion only, i.e., advection in the matrix is neglected.
- Diffusion is one-dimensional from the fracture into the rock matrix, where transverse fluxes (i.e., diffusive fluxes parallel to the fracture plane) are neglected.
- The mass flux in the fracture is due to advection only.
- Fully mixed conditions prevail in the streamtube in the direction orthogonal to the fracture plane.

The above assumptions are similar to those used in previous transport models [*Foster*, 1975; *Grisak and Pickens*, 1980; *Neretnieks*, 1980; *Moreno et al.*, 1985; *Cvetkovic et al.*, 1999].

Cumulative arrival time for reacting tracers

Under the assumptions given in section 2.3, the time-dependent concentration in the fracture and the related tracer flux in the flow direction have closed-form solutions. For example, the flux response function, defined as the tracer flux at the fracture outlet due to a unit impulse (δ-function) injection of mass at $t = 0$, is [*Cvetkovic et al.*, 1999]

$$R(t;\tau,\beta) = \frac{H(t-\tau-K_d^f\beta)\kappa\beta}{2\sqrt{\pi}(t-\tau-K_d^f\beta)^{3/2}}\exp\left[\frac{-\kappa^2\beta^2}{4(t-\tau-K_d^f\beta)}\right]. \tag{1}$$

Here $\kappa = \theta\sqrt{DR_m}$, θ is the matrix porosity, $R_m = 1 + K_d^m$, K_d^m (K_d^f) is the distribution coefficient for sorption in the matrix (surface), D is the matrix diffusion coefficient, and H the unit step function. The fluid residence time in the pathway is

$$\tau = \sum_1^n \tau_i = \frac{1}{Q}\sum_1^n \int_0^{l_i} b_i(x_i)w_i(x_i)dx_i \tag{2}$$

and the specific contact surface is

$$\beta = \sum_1^n \beta_i = \frac{1}{Q}\sum_1^n \int_0^{l_i} w_i(x_i)dx_i. \tag{3}$$

If internal variability is neglected,

$$\tau = \sum_{i=1}^n \tau_i = \frac{w_0}{Q}\sum_1^n l_i\bar{b}_i \tag{4}$$

$$\beta = \sum_{i=1}^n \beta_i = \frac{w_0}{Q}\sum_1^n l_i. \tag{5}$$

The time of arrival t_ϕ for the cumulative mass fraction ϕ is another effect of interest that is convenient in some applications. This is easily derived from equation 1 and provides a more condensed summary of the retention properties of the fractured rock mass. After integrating (1), we find

$$t_\phi = \tau + \frac{\kappa^2}{4F^2}\beta^2 \tag{6}$$

where $F(\phi)$ is the inverse of the complementary error function, defined implicitly as $\zeta = F(\phi)$ with

$$\phi = \frac{2}{\sqrt{\pi}}\int_\zeta^\infty \exp\left[-t^2\right]\,dt. \tag{7}$$

Equations (4) to (6) form the basis of our analysis. We are interested in the expected value and uncertainty in t_ϕ in the situation in which the aperture and length are unobserved but have known joint density function.

Stochastic analysis of a multiple-fracture pathway

The flux response function (equation (1)) and related quantities such as t_ϕ depend on the pathway τ and β, which are random variables due to their dependence on the random variables, L_i and B_i, representing the unobserved lengths and apertures. In [*Painter et al.*, 1998] we outlined a procedure for calculating the statistics of τ and β given the statistics of the length and aperture.

This procedure relates the individual fracture attributes, τ_1, β_1, to those for the entire pathway, τ, β, through an n-fold convolution,

$$\tilde{f}_{\beta,\tau}(\nu,\omega) \;=\; [\tilde{f}_{\beta_1,\tau_1}(\nu,\omega)]^n. \tag{8}$$

Here $\tilde{f}_{\beta,\tau}$ is the characteristic function (Fourier transform of the density function) of β, τ, and ν, ω are the corresponding fourier variables. Recall that we have assumed independent and identically distributed segments so that $f_{\beta_i,\tau_i}(\beta_i,\tau_i) \;=\; f_{\beta_j,\tau_j}(\beta_j,\tau_j)\ \forall\ i,j$; we use the subscript 1 to denote single fracture properties.

Equation (8) is a general result that does not depend on specific assumptions about the τ_1, β_1 distribution or even the existence of moments of the distribution. The only restriction is that the aperture/length pairs for individual segments are independent of other segments and identically distributed. If the full probability density function (pdf) is needed, it can be further related to the pdf for length and aperture [*Painter et al.*, 1998]. In the following discussion, we require only the moments of the τ, β distribution, not the full pdf. These moments can be related to length/aperture moments without knowing the details of the density function (see the Appendix). This presumes that the moments are finite, which excludes the situation of a power-law length distribution. The

consequences of a power-law length distribution are addressed in *Painter et al.* [1998].

Moments of the cumulative arrival time

The expected value of the cumulative arrival time (equation (6)) can be related to the moments of β, τ without reference to the full pdf $f_{\beta,\tau}(\beta,\tau)$. The expected value of t_ϕ is

$$\langle t_\phi \rangle = \langle \tau \rangle + \frac{\kappa^2}{4F^2}\langle \beta^2 \rangle \tag{9}$$

and the variance is

$$\sigma_{t_\phi}^2 = \sigma_\tau^2 + \frac{\kappa^2}{2F^2}\left[\langle \beta^2 \tau \rangle - \langle \beta^2 \rangle \langle \tau \rangle\right] + \frac{\kappa^4}{16F^4}\left[\langle \beta^4 \rangle - \langle \beta^2 \rangle^2\right]. \tag{10}$$

The moments for the arrival time can further be related to the moments for individual fracture aperture and length by using the relationships given in the Appendix. It is convenient to consider these moments in nondimensional form normalized by the deterministic nonreacting travel time

$$\tau_d = \frac{n}{q}\langle l_1 \rangle \langle \bar{b}_1 \rangle \tag{11}$$

where $q = Q/w_0$. This deterministic travel time is obtained by neglecting aperture and length variability and considering the multiple-fracture pathway to be a single fracture with length $n\langle l_1 \rangle$ and aperture $\langle \bar{b}_1 \rangle$. Using this normalization, we obtain for $n \gg 1$

$$\frac{\langle t_\phi \rangle}{\tau_d} = \frac{\langle l_1 \bar{b}_1 \rangle}{\langle l_1 \rangle \langle \bar{b}_1 \rangle} + \eta. \tag{12}$$

The dimensionless parameter

$$\eta = \frac{\eta_B}{4F^2} = \frac{\kappa^2 n \langle l_1 \rangle}{4F^2 q \langle \bar{b}_1 \rangle} \tag{13}$$

measures the importance of mass exchange processes relative to advection for the multiple-fracture pathway. Large values of η imply that the combined effects of diffusion and sorption dominate over advection, while the opposite is true for $\eta \ll 1$.

The parameter η is proportional to total length of the pathway $n\langle l_1\rangle$ and inversely proportional to the flow rate q.

The parameter η also depends nonlinearly on the cumulative mass fraction ϕ through the inverse complementary error function $F(\phi)$. η is larger and the retention processes more important for the trailing edge of the plume (ϕ near 1) as compared to the leading edge or bulk $\phi \simeq 1/2$. The importance of retention processes for the bulk of the plume is quantified by η_B, which is approximately $\eta|_{\phi=1/2}$. By varying ϕ and calculating the cumulative arrival time, it is possible to map out the expected value for the entire arrival time curve (arrival time t_ϕ at the outlet versus cumulative mass fraction ϕ). This is shown in Figure 3. The expected arrival time curve depends only on three parameters: τ_d, which serves as a normalization for time, $\langle l_1\bar{b}_1\rangle/\langle l_1\rangle\langle\bar{b}_1\rangle$, and η_B. This family of curves is particularly sensitive to η_B. The purely advective situation $\eta_B = 0$ results in an expected arrival time curve independent of ϕ with magnitude $\langle l_1\bar{b}_1\rangle/\langle l_1\rangle\langle\bar{b}_1\rangle$. For larger values of η_B, downstream particle movement is slowed by the retention processes, and the expected arrival time increases in magnitude.

Equations (12) and (13) are two of the key results of this paper. They show how the expected arrival time is enhanced over the deterministic nonreacting arrival time by retention processes, quantified through the dimensionless parameter η, and by length-aperture correlation, quantified by the first term in equation (12). The normalized moment in the first term is unity in the situation of no correlation between length and aperture. It is less than one when negative correlations exist. However, positive correlation between fracture lengths and apertures is the general rule, and this term is greater than 1, indicating an enhancement in the expected arrival time relative to the deterministic value. This generic result has some immediate consequences for analysis of transport in fractured rock. Simplified analyses that neglect spatial variability in fracture attributes may result in a *systematic bias* in the predicted result.

Although length and aperture variability around the expected values have no effect

on $\langle t_\phi \rangle$ when the length and apertures are uncorrelated, the same is not true for the variance in the arrival time. Using equation (10) and the results in the Appendix,

$$\frac{\sigma_{t_\phi}^2}{\tau_d^2} = \frac{1}{n}\left[\frac{\langle l_1^2\bar{b}_1^2\rangle - \langle l_1\bar{b}_1\rangle^2}{\langle l_1\rangle^2\langle\bar{b}_1\rangle^2} + 4\eta\frac{\langle l_1^2\bar{b}_1\rangle - \langle l_1\rangle\langle l_1\bar{b}_1\rangle}{\langle l_1\rangle^2\langle\bar{b}_1\rangle} + 4\eta^2\frac{\sigma_{l_1}^2}{\langle l_1\rangle^2}\right]. \tag{14}$$

Here, as in equation (12), terms of order $1/n$ have been neglected relative to unity. This approximation is appropriate as typical applications would have $n \gg 1$. The variance in the predicted arrival time decreases as $1/n$, increases nonlinearly with increasing η, and also depends on three sets of normalized moments that quantify length variability and length-aperture correlation.

Results using a log-normal distribution

The log-normal distribution is probably the most frequently used distribution for modeling fracture apertures and lengths. Usually, correlation between aperture and length is ignored, even though it is well established from laboratory and field studies (see e.g. *Barton and Zoback* [1996]) that aperture and length have a strong positive correlation. In this section, the formalism outlined in the previous sections is applied to the log-normal situation. In addition, we retain the correlation between aperture and length to assess its effect.

Consider a bivariate log-normal distribution for aperture $\bar{b}_1$ and length l_1 for individual fractures:

$$\begin{aligned} f_{L_1,B_1}(l_1,\bar{b}_1) &= \ell n(l_1,\bar{b}_1\ ;\ l_g, b_g, \Sigma) \\ &= \frac{1}{2\pi l_1\bar{b}_1\,|\Sigma|^{1/2}}\exp\left[-\frac{1}{2}\begin{pmatrix}\ln(l_1/l_g)\\ \ln(\bar{b}_1/b_g)\end{pmatrix}^T \Sigma^{-1}\begin{pmatrix}\ln(l_1/l_g)\\ \ln(\bar{b}_1/b_g)\end{pmatrix}\right] \end{aligned}$$

where b_g and l_g are geometric means for aperture and length and Σ is the co-variance matrix for $\ln\bar{b}_1$ and $\ln l_1$. Correlation between aperture and length is included in this model through the off-diagonal term Σ_{12}.

Using the bivariate log-normal model for l_1 and $\bar{b}_1$ and standard results on the moments for log-normal variables, the expected value of the cumulative arrival time is calculated from equation (12) as

$$\frac{\langle t_\phi \rangle}{\tau_d} = \exp\left[\rho \sigma_{\ln l_1} \sigma_{\ln \bar{b}_1}\right] + \eta, \tag{15}$$

where ρ is the correlation coefficient between $\ln l_1$ and $\ln b_1$. Taking $\sigma_{\ln l_1} = \sigma_{\ln \bar{b}_1} = 1$ as typical values, the first term on the right varies from 0.37 for $\rho = -1$ to 0 for $\rho = 0$ to 2.72 for $\rho = 1$. This demonstrates the potentially large error that can be incurred by neglecting correlation between length and aperture. This error is less important when retention dominates $\eta > 1$.

The variance in the arrival time is obtained in a similar manner as

$$\begin{aligned} n\frac{\sigma^2_{t_\phi}}{\tau_d^2} &= A_0 + 4A_1\eta + 4A_2\eta^2 \\ A_0 &= \exp\left[\sigma^2_{l_1} + 4\rho\sigma_{l_1}\sigma_{\bar{b}_1} + \sigma^2_{\bar{b}_1}\right] - \exp\left[2\rho\sigma_{l_1}\sigma_{\bar{b}_1}\right] \\ A_1 &= \exp\left[\sigma^2_{l_1} + 2\rho\sigma_{l_1}\sigma_{\bar{b}_1} + \sigma^2_{\bar{b}_1}\right] - \exp\left[\rho\sigma_{l_1}\sigma_{\bar{b}_1}\right] \\ A_2 &= \exp\left[\sigma^2_{l_1}\right] - 1 \end{aligned} \tag{16}$$

Examples of arrival time curves with uncertainty are shown in Figure 4. In each plot, the three curves represent the expected value of the arrival time curve plus/minus one standard deviation. The parameters used here are $\sigma_{\ln l_1} = \sigma_{\ln \bar{b}_1} = 1$, $\eta_B = 1$, and $n = 50$. Figure 4a has $\rho = 0$, while Figures 4b and 4c have $\rho = -3/4$ and $\rho = 3/4$, respectively. Positive correlations shift the arrival time curves to longer times but also dramatically increase the uncertainty in the arrival time curve, once again demonstrating the need to include correlations between the fracture apertures and lengths. The asymmetry in the sensitivity to ρ is a result of the right-skewed nature of the log-normal distribution.

Similar comparisons can be used to study the relative sensitivity to length and aperture variability. Using the same set of parameters as in Figure 4a and fixing $\phi = 0.5$,

$\langle t_\phi \rangle / \tau_d = 2.10$ and $\sigma^2_{t_\phi}/\tau_d^2 = 0.44$. The expected value is independent of length/aperture variability in this case because $\rho = 0$, but $\sigma^2_{t_\phi}/\tau_d^2$ depends on both. Decreasing $\sigma_{\ln l_1}$ to 0.5 while holding $\sigma_{\ln \bar{b}_1} = 1$ decreases $\sigma^2_{t_\phi}/\tau_d^2$ to 0.10. Switching the values for $\sigma_{\ln l_1}$ and $\sigma_{\ln \bar{b}_1}$ results in $\sigma^2_{t_\phi}/\tau_d^2 = 0.36$. This comparison demonstrates that aperture variability is less important than length variability in determining the uncertainty in the arrival time curves. This may seem counterintuitive because the transmissivity of fractures and thus the flow are known to be sensitive to the fracture aperture. The reason for the reduced sensitivity to aperture is that we have fixed the volumetric flow rate Q instead of the applied macroscopic gradient. More complicated situations with a fixed macroscopic gradient and a resulting uncertain flow rate have been analyzed. These situations will be summarized in a future paper.

Effect of Uncertainty in the Volumetric Flow Rate

One important parameter appearing in the analysis is Q, the volumetric discharge through the streamtube. This quantity is constant through the streamtube and appears in the bulk retention parameter η_B and the groundwater travel time τ_D. The volumetric flowrate Q was treated as a deterministic quantity in the preceding analysis. However, the analysis can be extended to allow for uncertainty in Q. Whether it is more appropriate to treat Q deterministically or statistically depends on the situation being analyzed. If the most likely pathway from the repository engineered system is known *a priori* from site investigations, then it is appropriate to treat Q deterministically. If not, then it is appropriate to treat it stochastically. In this case, the Q statistics may be determined from network simulations or from borehole packer tests during the site investigation stage.

Equations (12) and (14) are easily extended to treat the situation of an uncertain Q. In this case the deterministic Q appearing in the bulk retention parameter η_B and groundwater travel time τ_D is replaced by the expected flow rate $\langle Q \rangle$. The expected

arrival time becomes

$$\frac{\langle t_\phi \rangle}{\tau_d} = \langle Q^{-1} \rangle \langle Q \rangle \frac{\langle l_1 \bar{b}_1 \rangle}{\langle l_1 \rangle \langle \bar{b}_1 \rangle} + \left[\langle Q^{-1} \rangle \langle Q \rangle \right]^2 \eta. \tag{17}$$

Note that quantity $[\langle Q^{-1} \rangle \langle Q \rangle]$ can be larger or small than unity, depending on the Q distribution. If Q has a uniform distribution, the quantity is less than one. If Q has a log-normal distribution, the quantity is greater than one. Thus, deterministic estimates of arrival time obtained by replacing Q with expected volumetric flow rate $\langle Q \rangle$ may contain a systematic bias compared to the properly averaged arrival time. It should be noted that this reduction in the effective retention is not due to spatial variability; Q is still constant along the flowpath. It is due instead to the nonlinear nature of the retention process which causes the small Q part of the distribution to contribute more to the expected arrival time. The effect of Q uncertainty on the arrival time variance can be quantified in an analogous way.

Effects of Internal Variability in Fracture Aperture

The results in the previous sections neglected within-fracture aperture variability and focused on the effects of fracture-to-fracture variability. In this section, the framework is extended to include both fracture-to-fracture and within-fracture variability.

A variety of models for flow and transport in individual fractures has been developed. The earliest approaches [*Snow*, 1965] used a spatially constant parallel plate model with laminar flow in which the resistance to flow is inversely proportional to the aperture cubed (cubic law). At the next level of complexity, a fracture is modeled as a bond (channel) network [*Neuzil and Tracy*, 1981; *Neretnieks*, 1983] with fracture aperture (or velocity) varying randomly from channel to channel. This model mimics the tendency toward "channelization" of flow in spatially variable fractures. As a further refinement of single-fracture models, the aperture may be considered a random space

function (RSF) with the cubic law applicable locally [*Moreno et al.*, 1988; *Tsang and Tsang*, 1989]. Analytical results for tracer arrival time have also been obtained using this variable aperture model [*Cvetkovic*, 1991], the most recent of which [*Cvetkovic et al.*, 1999] utilizes the Lagrangian framework for transport in aquifers [*Cvetkovic and Dagan*, 1994; *Dagan and Cvetkovic*, 1996; *Cvetkovic and Dagan*, 1996] to account for matrix diffusion and rate-limited sorption in addition to advection.

Local variability in the fracture apertures causes the flowpath to meander through the fracture plane and the flowpath width w to fluctuate along the flowpath trajectory. Cvetkovic *et al.* [1999] employed a log-normal RSF model for streamtube width/aperture variability in a single fracture. We merge this model with our shifting-mean model (Figure 2) and use the following model for width and aperture in fracture i:

$$b_i(x_i) = b_{gi} \exp\left[Y_i(x_i)\right] \tag{18}$$

$$w_i(x_i) = w_{gi} \exp\left[AY_i(x_i) + Z_i(x_i)\right] \tag{19}$$

where Y_i and Z_i are independent, normally distributed RSFs with zero mean and given covariance,

$$\langle Y_i(x_i) Y_i(x_i') \rangle = C_Y(r\ ;\ a_Y) \tag{20}$$

where $r = |x_i - x_i'|$ and $C(r; a)$ is a valid covariance function characterized by the correlation length a_Y. The parameter A in equation (19) accounts for correlation between the local width and aperture. Positive A implies positive correlation, $A = 0$ implies no correlation, and negative A implies negative correlation. The correlation coefficient between w and b depends on A and also on σ_Y and σ_Z. We make the correlation length a fixed fraction of the segment length l_i so that

$$C_Y(r\ ;\ a_Y) = C_Y(\xi\ ;\ a_Y') \tag{21}$$

where $\xi = r/l_i$ and $a_Y' = a_Y/l_i$ is the same for all i. We also assume that $\sigma_Y^2 = C_Y(0)$ is the same for all fractures.

The geometric mean b_{gi} appearing in equation (19) can be different for each fracture in the fracture chain. Moreover, these moments are only known statistically. Using standard relationships for the means of log-normal variables, the geometric mean b_{gi} and effective aperture $\bar{b}_i$ are related

$$\bar{b}_i = b_{gi} \exp\left[\frac{\sigma_Y^2}{2}\right] \tag{22}$$

$$w_0 = w_g \exp\left[A^2\frac{\sigma_Y^2}{2} + \frac{\sigma_Z^2}{2}\right] \tag{23}$$

As before, we model the length l_i and average aperture $\bar{b}_i$ as random variables.

Moments of β_i, τ_i within a single fracture were derived by Cvetkovic *et al.* [1999]. These can be regarded as conditional moments $\langle \beta_i^m \tau_i^p \mid l_i, \bar{b}_i \rangle$. The first few moments for use in $\langle t_\phi \rangle$ are

$$\langle \beta_i \mid l_i, \bar{b}_i \rangle = \frac{w_g l_i}{Q} \exp\left[A^2\frac{\sigma_Y^2}{2} + \frac{\sigma_Z^2}{2}\right] = \frac{w_0 l_i}{Q} \tag{24}$$

$$\langle \tau_i \mid l_i, \bar{b}_i \rangle = \frac{b_{gi} w_g l_i}{Q} \exp\left[\frac{(A+1)^2\sigma_Y^2}{2} + \frac{\sigma_Z^2}{2}\right] \tag{25}$$

$$= 2\frac{\bar{b}_i w_0 l_i}{Q} \exp\left[A\sigma_Y^2\right] \tag{26}$$

$$\langle \beta_i^2 \mid l, \bar{b}_i \rangle = \frac{w_0^2 l_i^2}{Q^2} \int_0^1 (1-\xi) \exp\left[A^2 C_Y(\xi; a'_Y) + C_Z(\xi; a'_Z)\right] d\xi. \tag{27}$$

Within the present shifting-mean model, moments of β_1, τ_1 are obtained from these conditional moments as

$$\langle \beta_i^m \tau_i^p \rangle = \int_0^\infty \int_0^\infty \langle \beta_i^m \tau_i^p \mid l_i, \bar{b}_i \rangle f_{L_i, \bar{B}_i}(l_i, \bar{b}_i)\, dl_i\, d\bar{b}_i. \tag{28}$$

The moments appearing in the expression for $\langle t_\phi \rangle$ are

$$\langle \beta_i \rangle = \frac{\langle l_i \rangle w_0}{Q} \tag{29}$$

$$\langle \beta_i^2 \rangle = \frac{2\langle l_i^2 \rangle w_0^2}{Q^2} \int_0^1 (1-\xi) \exp\left[A^2 C_Y(\xi; a'_Y) + C_Z(\xi; a'_Z)\right] d\xi \tag{30}$$

$$\langle \tau_i \rangle = \frac{\langle \bar{b}_i l_i \rangle}{q} \exp\left[A\sigma_Y^2\right]. \tag{31}$$

Thus, the internal variability acts to enhance the moments of τ_1, β_1 relative to the situation without internal variability.

Combining these moments, equation (9), and the results in the Appendix, we obtain the following result for the expected value for arrival time including internal and fracture-to-fracture variabilities

$$\frac{\langle t_\phi \rangle}{\tau_d} = \frac{\langle l_1 \bar{b}_1 \rangle}{\langle l_1 \rangle \langle \bar{b}_1 \rangle} \exp\left[A\sigma_Y^2\right] + \eta. \tag{32}$$

The only difference between this and the corresponding result without internal aperture variability is the term $\exp[A\sigma_Y^2]$. Thus, internal aperture variability decreases the expected arrival time when $A < 1$ and increases it when $A > 1$, where A is the parameter quantifying local correlation in width and aperture of the local flowpath (see the discussion following equation (19)).

The corresponding result for the variance in arrival time is

$$\begin{aligned} n\frac{\sigma_{t_\phi}^2}{\tau_d^2} &= \exp\left[2A\sigma_Y^2\right] \frac{\langle l_1^2 \bar{b}_1^2 \rangle I_1 - \langle l_1 \bar{b}_1 \rangle^2}{\langle l_1 \rangle^2 \langle \bar{b}_1 \rangle^2} + 4\eta \exp\left[A\sigma_Y^2\right] \frac{\langle l_1^2 \bar{b}_1 \rangle I_2 - \langle l_1 \rangle \langle l_1 \bar{b}_1 \rangle}{\langle l_1 \rangle^2 \langle \bar{b}_1 \rangle} \\ &\quad + 4\eta^2 \frac{\langle l_1^2 \rangle I_3 - \langle l_1 \rangle^2}{\langle l_1 \rangle^2}. \end{aligned} \tag{33}$$

where

$$I_1 = 2\int_0^1 (1-\xi) \exp\left[(A+1)^2 C_Y(\xi) + C_Z(\xi)\right] d\xi \tag{34}$$

$$I_2 = 2\exp\left[-\frac{1}{2}\sigma_Y^2\right] \int_0^1 (1-\xi) \exp\left[(A+1)AC_Y(\xi) + C_Z(\xi)\right] d\xi \tag{35}$$

$$I_3 = 2\int_0^1 (1-\xi) \exp\left[A^2 C_Y(\xi) + C_Z(\xi)\right] d\xi \tag{36}$$

Note that σ_{t_ϕ} depends strongly on A and σ_Y, is less sensitive to the normalized correlation functions C_Y and C_Z, and is completely independent of the parameter σ_Z.

In our parameterization of the streamtube fluctuations inside individual fractures, we treated the quantities A, σ_Y, σ_Z, C_Z, and C_Y as independent parameters. In reality, these quantities are not independent since width and aperture fluctuations are linked

through the equations describing flow in the fractures. Ultimately, all these quantities are controlled by the aperture variations. Cvetkovic *et al.* [1999] addressed this issue through numerical simulation of flow in individual fractures with variable apertures. Analysis of these simulations suggests $A \approx -1.4$. This result is independent of σ_Y and C_Y and is believed to be a consequence of the cubic law for fracture flow.[1] Analysis of the single-fracture simulations also reveals a strong relationship between σ_Y and σ_Z, which is immaterial in the present context since equations (32) and (33) are independent of σ_Z.

Using $A = -1.4$, it is seen that internal variability in fracture apertures decreases the expected arrival time. The magnitude of this decrease depends on the value of η, and σ_Y^2. In the advection-dominated case ($\eta_B \ll 1$) or when focusing on the early arrivals ($\phi \ll 1$), this factor is approximately 0.70 when $\sigma_Y^2 = 0.25$. That is, the expected arrival time is reduced by about 30 percent by internal variability. This modest bias introduced by neglecting internal variability is significantly smaller in relative terms if the focus is on the bulk arrival time $\phi \approx 1/2$ or if retention processes are significant $\eta_B \geq 1$. This is illustrated in Figure 5 using the log-normal example of Figure 4*c*. The solid curves are the expected arrival time plus or minus one standard deviation for the situation without internal variability. The dashed curves are the same including internal variability with $\sigma_Y^2 = 0.25$. For this example, internal variability reduces $\langle t_{1/2} \rangle / \tau_D$ from 3.22 to 2.59. Uncertainty in the arrival time is also reduced, but in relative terms the effect is small. These examples illustrate that the neglect of internal variability is an acceptable approximation in most applications, with the possible exception of advection dominated situations ($\eta \ll 1$).

---

[1]Different values of A may result if the local cubic law for fracture flow does not hold, as has been discussed by *Oron and Berkowitz* [1998].

Requirements for site-specific applications

Although this paper is concerned mainly with methodology and broad-scope generic analysis, the pathway model and analysis method also have potential for site-specific quantitative applications. However, some auxiliary simulations are necessary to relate some of the key quantities required in the analysis to those that are more readily measured in a site investigation. The required auxiliary calculations take the form of Monte Carlo simulations of discrete-fracture networks coupled with numerical solutions for hydraulic head and nonreacting tracer transport. These simulations may be done on a scale much smaller than the repository geosphere, and do not involve the mass exchange processes, which are more difficult to simulate in a discrete fracture model. The proposed approach, then, allows for systematic upscaling from modest fracture-network simulations to large-scale transport predictions involving significant mass retention.

Consider, for example, n, the number of fracture segments along the pathway. In general, this is not available directly in an application. The distance Δ from the release point to the compliance boundary is typically available instead. In this case, $n = \frac{\lambda\Delta}{\langle l_1 \rangle}$, where $\lambda \geq 1$ is a tortuosity factor for the network. This factor is not greatly different from unity for a well-connected network, but may be so for networks near the percolation threshold. The tortuosity factor may be determined, if it is needed precisely, through a set of fracture network simulations. Note that fixing n in this way does not fix precisely the total length traveled by the contaminants, as $l = \sum_1^n l_i$ remains a random variable.

A similar situation exists for the $l_i, \bar{b}_i$ statistics. These are not the fracture length and aperture statistics measured in the field, but the length and aperture for segments along the pathway. The distinction is similar to the distinction between Lagrangian and Eulerian velocities in a continuum-level stochastic model. Again these $l_i, \bar{b}_i$ statistics can be related to field-measured fracture and aperture statistics through network simulations, as just described.

Conclusions

In summary, we analyzed transport of reactive tracers in a set of fractures connected in series to form a pathway through otherwise impermeable rock. This idealized scenario is important in several contexts in subsurface environmental physics, with particular significance for studies of geological isolation of high-level nuclear waste. The novel features of this work are the coupling of mass exchange processes such as matrix diffusion and equilibrium sorption with large-scale fluctuations in advective velocities. Although the emphasis in this paper is on the general methodology and not applications, it is possible to draw some generic conclusions.

Perhaps the most useful result is the identification of the dimensionless retention parameter η defined in equation (13). This parameter quantifies the importance of advection relative to the combined effects of matrix diffusion and sorption, which act to retain particles in the host rock. This retention parameter combines expected values for the fracture attributes with the specific discharge rate and the sorption and diffusion properties of the host rock. The retention parameter is easily calculated from these quantities, which can be measured or estimated in site characterization studies, thus providing a simple global measure of likely retention in the host rock.

The main conclusion concerns the potential error that could be incurred by ignoring spatial variability in fracture attributes along a pathway. The results for the expected flux and expected arrival time clearly show that the prediction will contain a systematic bias if this variability is ignored. The only situation in which this bias is not present is when the fracture lengths and apertures are completely uncorrelated. Positive correlation between fracture lengths and apertures, the usual situation, results in later arrival times compared with the deterministic estimate obtained by ignoring variability. However, that is not to say that the deterministic estimate is conservative. Indeed, the standard deviation in the flux or travel time estimates can be quite large, even for modest values for n, the total number of fracture segments. Thus, the true arrival time

may be larger or smaller than the deterministic estimate.

Our results also provide some understanding of the relative sensitivities that can be used to guide site characterization studies. If n is large compared to unity, the expected arrival time depends on the correlation between length and aperture and on the retention parameter. Details of the length-aperture distribution beyond the lower moments are unimportant. The variance in the arrival time depends more strongly on the retention parameter and also on the other lower moments of the length-aperture distribution. Moreover, the variance depends more strongly on length distribution as opposed to the aperture distribution. Thus, site characterization should concentrate on the parameters entering the retention parameter and on the lower moments of fracture length and aperture.

These sensitivities depend on a spatially constant matrix diffusion and sorption parameters and finite second moment for the length distribution. If any one of these assumptions are violated, the sensitivities may be different. The situation of a power-law distribution for fracture lengths has already been studied [*Painter et al.*, 1998].

The final conclusion concerns the use of analytical methods for predictive studies of transport away from a geological waste repository. Clearly, methods such as those developed here do not provide the level of detail and the fidelity to the physical processes that complex numerical models can provide. They are intended to provide simple, transparent, and reproducible complements to numerical models, thereby guiding the application and understanding of computational studies. A major advantage of our analytical approach is that it treats uncertainty in an explicit manner without requiring Monte Carlo simulations. Some of the simplifying assumptions may be removed by coupling to relatively simple network simulations. This hybrid approach is particularly appealing. It may provide a practical, yet accurate, method for risk-based assessment of repository geosphere performance.

Appendix A: Moments of τ and β

The arrival time moments depend on the moments of τ and β, which depend in turn on length and aperture moments. From the definition of the τ_i and β_i, the moments of the single-fracture attributes are

$$\langle \tau_i \rangle = \frac{1}{q} \langle l_1 \bar{b}_i \rangle \tag{A1}$$

and

$$\langle \beta_i \rangle = \frac{1}{q} \langle l_1 \rangle. \tag{A2}$$

Note that $\langle \beta_1 \rangle = \langle \beta_i \rangle \ \forall i$ since each length/aperture pair is identically distributed.

The next step is to relate the pathway τ, β to the individual fracture attributes τ_1, β_1. This is accomplished using equation (8) and standard relationships between the moments and characteristic function. In general, the finite moments of the random vector (X,Y) are related to its characteristic function via

$$\langle X^p Y^m \rangle = \imath^{-m-p} \frac{\partial^p \partial^m}{\partial \nu^p \partial \omega^m} \tilde{f}_{X,Y}(\nu, \omega) \Big|_{\nu,\omega=0} \tag{A3}$$

Applying this relationship between moments and characteristic function to equation 8,

$$\langle \tau^p \beta^m \rangle = \imath^{-p-m} \frac{\partial^p \partial^m}{\partial \nu^p \partial \omega^m} [\tilde{f}_{\tau_1,\beta_1}(\nu, \omega)]^n \Big|_{\nu,\omega=0}. \tag{A4}$$

Arbitrary moments of β, τ can be generated in this way by repeated application of the differentiation operator and by using

$$\tilde{f}_{\tau_1,\beta_1}(\nu, \omega) \Big|_{\nu,\omega=0} = 1, \tag{A5}$$

which is the Fourier-domain equivalent to the usual normalization condition for probability density functions.

The first few non-centered moments obtained in this way are

$$\langle \tau \rangle = n \langle \tau_1 \rangle \tag{A6}$$

$$\langle\beta\rangle = n\langle\beta_1\rangle \tag{A7}$$

$$\langle\beta^2\rangle = n\langle\beta_1^2\rangle + n(n-1)\langle\beta_1\rangle^2 \tag{A8}$$

$$\langle\tau\beta\rangle = n\langle\tau_1\beta_1\rangle + n(n-1)\langle\tau_1\rangle\langle\beta_1\rangle \tag{A9}$$

$$\begin{aligned}\langle\tau\beta^2\rangle = {} & n\langle\tau_1\beta_1^2\rangle + n(n-1)\langle\tau_1\rangle\langle\beta_1\rangle + \\ & 2n(n-1)\langle\beta_1\rangle\langle\beta_1\tau_1\rangle + n(n-1)(n-2)\langle\beta_1\rangle^2\langle\tau_1\rangle\end{aligned} \tag{A10}$$

$$\begin{aligned}\langle\beta^4\rangle = {} & n\langle\beta_1^4\rangle + 4(n-1)n\langle\beta_1^3\rangle\langle\beta_1\rangle + \\ & 3(n-1)n\langle\beta_1^2\rangle^2 + 6(n-2)(n-1)n\langle\beta_1^2\rangle\langle\beta_1\rangle^2 + \\ & (n-3)(n-2)(n-1)n\langle\beta_1\rangle^4\end{aligned} \tag{A11}$$

while the centered moments appearing in equation (10) are

$$\sigma_\tau^2 = \langle\tau^2\rangle - \langle\tau\rangle^2 = n\sigma_{\tau_1}^2 \tag{A12}$$

$$\begin{aligned}&\left\langle\beta^2\tau\right\rangle - \left\langle\beta^2\right\rangle\langle\tau\rangle = \\ &\quad n\left[\left\langle\beta_1^2\tau_1\right\rangle - \left\langle\beta_1^2\right\rangle\langle\tau_1\rangle\right] + 2n(n-1)\left[\langle\beta_1\rangle\langle\beta_1\tau_1\rangle - \langle\beta_1\rangle^2\langle\tau_1\rangle\right]\end{aligned} \tag{A13}$$

$$\begin{aligned}\left\langle\beta^4\right\rangle - \left\langle\beta^2\right\rangle^2 = {} & n\left\langle\beta_1^4\right\rangle + 4(n-1)(n)\left\langle\beta_1^3\right\rangle\langle\beta_1\rangle + n(2n-1)\left\langle\beta_1^2\right\rangle^2 \\ & +4n(n-1)(n-3)\left\langle\beta_1^2\right\rangle\langle\beta_1\rangle^2 + 2n(n-1)(3-2n)\langle\beta_1\rangle^4\end{aligned} \tag{A14}$$

It is easily shown that the asymmetry parameter defined as the ratio of third centered moment to $\sigma^{3/2}$ decreases as $1/\sqrt{n}$ for large n. This relationship is consistent with the central limit theorem, which requires the distribution of τ, β to tend to a bi-variate Normal distribution as n becomes large.

Notation

a_Y Integral scale for C_Y.

$b_i(x_i)$ Aperture variations in the ith fracture segment.

$\bar{b}_i$ Spatial mean aperture in the ith fracture segment.

C_Y Covariance function for Y.

C_Z Covariance function for Z.

D Diffusion coefficient for solutes in the host rock.

$f_{\beta,\tau}$ Joint probability density function for β, τ.

f_{β_i,τ_i} Joint probability density function for β_i, τ_i.

f_{L_1,B_1} Joint probability density function for length and aperture.

$F(\cdot)$ Inverse of the complementary error function.

K_d^m Equilibrium distribution coefficient for sorption in the host rock.

K_d^f Equilibrium distribution coefficient for sorption on the fracture surface.

l_i Length of the ith fracture segment.

$\ell n(\cdot)$ Log-normal probability density function.

n Number of fractures in the multiple-fracture pathway.

q Q/w_0.

Q Volumetric flow rate.

$R(t\ ;\ \tau, \beta)$ Flux response function; flux at outlet of nth fracture due to δ-function input at $t = 0$.

R_m Retardation coefficient $1 + K_d^m$.

t_ϕ Time-of-arrival for the mass fraction ϕ.

$w_i(x_i)$ Streamtube width variations in the ith fracture segment.

w_0 Streamtube width at the initial release point.

Y_i Random space function used to describe aperture variability inside individual fractures (eq (18)).

Z_i Random space function used to describe flowpath width variability inside

individual fractures (eq (19)).

$\beta = \sum_1^n \beta_i$ Specific reactive surface area in the multiple-fracture pathway (eq (5)).

β_i Specific reactive surface area in the ith fracture.

η Retention parameter (eq (13)).

κ $\theta D/R_m$.

ρ Correlation coefficient between $\ln l_1$ and $\ln \bar{b}_i$ appearing in the log-normal model.

$\sigma_{\ln l_1}$ Standard deviation of $\ln l_1$, where l_1 is the length of individual segments.

$\sigma_{\ln \bar{b}_1}$ Standard deviation of $\ln \bar{b}_1$, where $\bar{b}_1$ is the individual segment apperture.

σ_Y^2 Variance of Y.

σ_Z^2 Variance of Z.

$\tau = \sum_1^n \tau_i$ Non-reacting travel time in the multiple-fracture pathway (eq (4)).

τ_d Deterministic non-reacting travel time (eq (11)).

τ_i Non-reacting travel time in the ith fracture.

θ Matrix porosity.

Acknowledgments.

This paper documents work performed in part by the Center for Nuclear Waste Regulatory Analyses for the Nuclear Regulatory Commission under contract NRC-02-97-009. This paper is an independent product and does not necessarily reflect the views or regulatory position of the NRC. This work was also supported in part by the Commonwealth Scientific and Industrial Research Organization (CSIRO). The authors are grateful to Dr. Lincoln Paterson of CSIRO and Dr. Jan-Olof Selroos of the Swedish Nuclear Fuel and Waste Management Company for their insights, and to Drs. B. Sagar and D. Hughson for their careful review of the manuscript.

References

Andersson, J., and B. Dverstorp, Conditional simulation of fluid flow in three-dimensional networks of discrete fractures, *Water Resour. Res.*, *23*, 1876–1886, 1987.

Barten, W., Linear response concept combining advection and limited rock matrix diffusion in a fracture network transport model, *Water Resour. Res.*, *32*, 3285–3296, 1996.

Barton, C. A., and M. D. Zoback, Self-similar distributions and properties of macroscopic fractures and depth in crystalline rock in the cajon pass scientific drill hole, *J. Geophysical Res.*, *97*, 5181–5200, 1996.

Berkowitz, B., J. Bear, and C. Braester, Continuum models for contaminant transport in fractured porous formations, *Water Resour. Res.*, *24*, 1225–1236, 1988.

Bibby, R., Mass transport of solutes in dual-porosity media, *Water Resour. Res.*, *17*, 1075–1081, 1981.

Birkholzer, J., H. Rubin, H. Daniels, and G. Rourve, Contaminant advection and spreading in a fractured permeable formation, 2, numerical simulation, *J. Hydrology*, *144*, 35–38, 1993.

Cacas, M. C., E. Ledoux, G. de Marsily, A. Barbreau, P. Calmels, B. Gaillard, and R. Margritta, Modeling fracture flow with a stochastic discrete fracture network: Calibration and validation, 2. the transport model, *Water Resour. Res.*, *20*, 491–500, 1990.

Cvetkovic, V., Mass arrival of reactive solute in a single fractures, *Water Resour. Res.*, *27*, 177–183, 1991.

Cvetkovic, V., and G. Dagan, Transport of kinetically sorbing solutes by steady random velocity in heterogeneous porous formations, *J. Fluid Mech.*, *265*, 189–215, 1994.

Cvetkovic, V., and G. Dagan, Reactive transport and immiscible flow in geological media 2: Applications, *Proceedings, Royal Society of London*, *452*, 303–328, 1996.

Cvetkovic, V., J. O. Selroos, and H. Cheng, Transport of reactive tracers in rock fractures, *J. Fluid Mech.*, *378*, 335–356, 1999.

Dagan, G., *Flow and Transport in Porous Formations*, Springer-Verlag, New York, 1989.

Dagan, G., and V. Cvetkovic, Reactive transport and immiscible flow in geological media 1: General theory, *Proceedings, Royal Society of London*, *452*, 285–301, 1996.

Dagan, G., and A. Fiori, The influence of of pre-scale dispersion on concentration statistical moments in transport through heterogeneous aquifers, *Water Resour. Res.*, *33*, 1997.

Dverstorp, B., J. Anderson, and W. Nordqvist, Discrete fracture network interpretation of field tracer tracer migration in sparsely fractured rock, *Water Resour. Res.*, *28*, 2327–2343, 1992.

Foster, S. S. D., The chalk groundwater tritium anomaly – a possible explanation, *J. Hydrology*, *25*, 159–165, 1975.

Grisak, G. E., and J. F. Pickens, Solute transport through fractured media 1. the effect of matrix diffusion, *Water Resour. Res.*, *16*, 719–730, 1980.

Kupper, J. A., F. W. Schwartz, and P. M. Steffler, A comparison of fracture mixing models, 1: A transfer function approach to mass transport modeling, *J. Contaminant Hydrology*, *18*, 1–32, 1995.

Long, J. C. S., J. S. Remer, C. R. Wilson, and P. A. Witherspoon, Porous media equivalents for networks of discontinuous fractures, *Water Resour. Res.*, *18*, 645–658, 1982.

Long, J. C. S., P. Gilmour, and P. A. Witherspoon, A model for steady fluid flow in random 3-d network of disc shaped fractures, *Water Resour. Res.*, *21*, 1105–1115, 1985.

Moreno, L., and I. Neretnieks, Fluid flow and solute transport in a network of channels, *J. Contaminant Hydrology*, *14*, 163–192, 1993.

Moreno, L., I. Neretnieks, and T. Eriksen, Analysis of some laboratory tracer runs in natural fissures, *Water Resour. Res.*, *21*, 951–958, 1985.

Moreno, L., Y. W. Tsang, C. F. Tsang, F. V. Hale, and I. Neretnieks, Flow and tracer transport in the a single fracture. a stochastic model and its relation to some field observations, *Water Resour. Res.*, *24*, 2033–2048, 1988.

Neretnieks, I., Diffusion in the rock matrix: An important factor in radionuclide retention, *J. Geophysical Res.*, *85*, 4379–4397, 1980.

Neretnieks, I., A note on fracture flow dispersion mechanisms in the ground, *Water Resour. Res.*, *19*, 364–370, 1983.

Neretnieks, I., Solute transport in fractured rock – applications to radionuclide waste repositories, in *Flow and contaminant transport in fractured rock*, Academic Press, San Diego, 1993.

Neuzil, C. E., and J. V. Tracy, Flow through fractures, *Water Resour. Res.*, *17*, 191–199, 1981.

Nordqvist, A. W., Y. M. Tsang, C. F. Tsang, B. Dverstorp, and J. Andersson, A variable aperture fracture network model for flow and transport in fractured rock, *Water Resour. Res.*, *28*, 1703–1713, 1992.

Oron, A., and B. Berkowitz, Flow in rock fractures: The local cubic law reexamined, *Water Resour. Res.*, *34*, 2811–2825, 1998.

Painter, S., V. Cvetkovic, and J.-O. Selroos, Transport and retention in fractured rock: Consequences of a power-law distribution for fracture lengths, *Physical Review E*, *57*, 6917–6922, 1998.

Pruess, K., and T. N. Narasimhan, A practical method for modeling fluid and heat flow in fractured porous media, *Soc. of Pet. Eng. J.*, *25*, 14–26, 1985.

Schwartz, F. W., L. Smith, and A. S. Crowe, A stochastic analysis of macroscopic dispersion in fractured media, *Water Resour. Res.*, *19*, 1253–1265, 1983.

Shapiro, A. M., and J. Andersson, Simulation of steady state flow in three-dimensional networks using the boundary element method, *Advances Water Resour.*, *8*, 106–110, 1985.

Smith, L., and F. W. Schwartz, An analysis of the influence of fracture geometry on mass transport in fracture media, *Water Resour. Res.*, *20*, 1241–1252, 1984.

Snow, D., A parallel plate model of fractured permeable media, Ph.D. thesis, University of California, Berkeley, 1965.

Tsang, Y. W., and C. F. Tsang, Flow channeling in a single fracture as a two-dimensional strongly heterogeneous permeable medium, *Water Resour. Res.*, *25*, 2076–2089, 1989.

S. Painter, Center for Nuclear Waste Regulatory Analyses, Southwest Research Institute, PO Drawer 28510, San Antonio, TX 78228-0510 (e-mail: spainter@swri.edu)

V. Cvetkovic, Division of Water Resources Engineering, Royal Institute of Technology, Stockholm, Sweden

Received _____

This manuscript was prepared with AGU's LaTeX macros v4, with the extension package 'AGU++' by P. W. Daly, version 1.6 from 1999/02/24.

Figure Captions

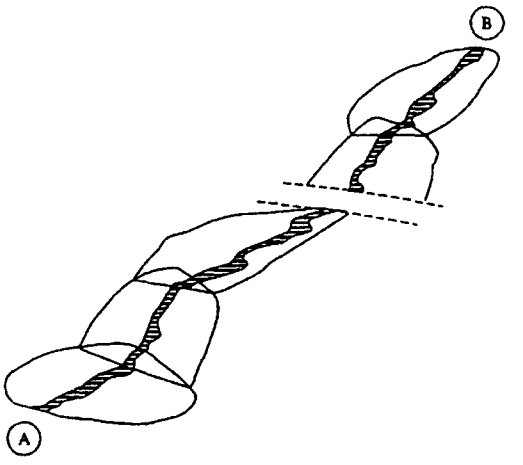

Figure 1. Transport pathway formed by multiple connected fractures in an otherwise impermeable medium. Fluid flowing at a constant volumetric rate through the fractures transports dissolved material by advection. The solute also diffuses into the stagnant pore fluid in the medium surrounding the fractures. Fracture lengths and apertures are unobserved with predefined joint probability density functions.

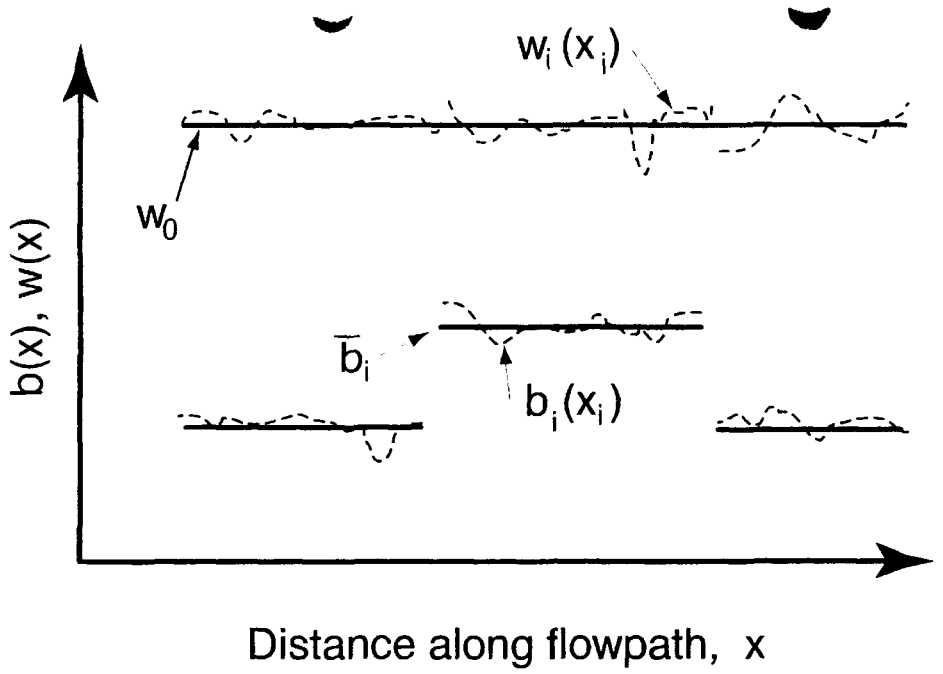

Figure 2. Shifting-mean model for aperture variation along a multiple fracture pathway. As the streamtube in Figure 1 passes from fracture to fracture, the local mean in the aperture undergoes stepwise changes. The segment means and segment lengths are modeled as random variables. In addition, the aperture may undergo local fluctuations within each segment. These are modeled as random space functions with specified spatial correlation structure.

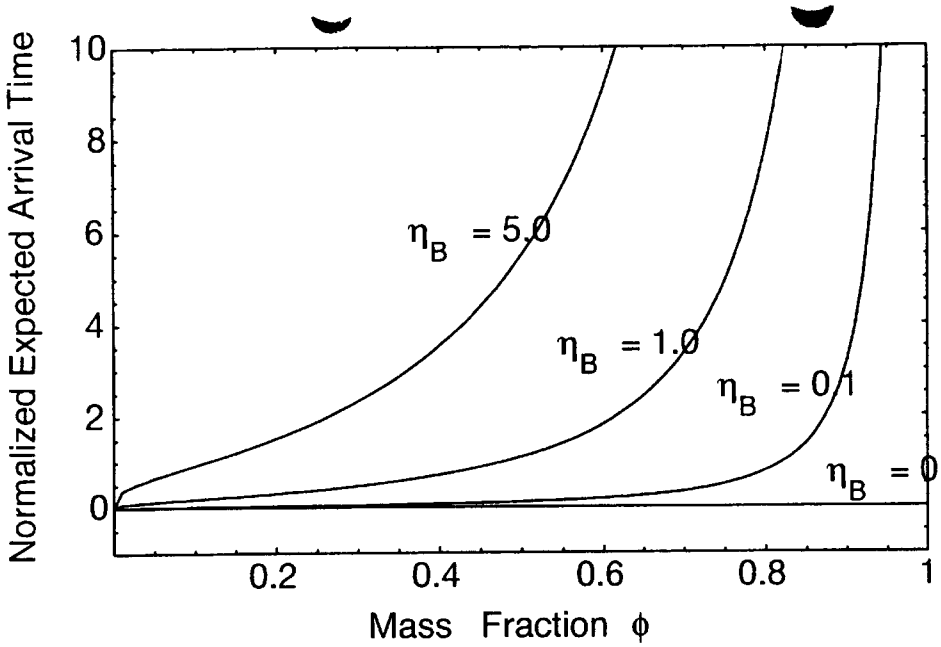

Figure 3. Expected values of normalized cumulative arrival time $\frac{\langle t_\phi \rangle}{\tau_d} - \frac{\langle l_1 b_1 \rangle}{\langle l_1 \rangle \langle b_1 \rangle}$ versus mass fraction ϕ for different values of the dimensionless bulk retention parameter η_B. In the shifted and normalized form of the expected arrival time used here, all parametric dependences are contained in the parameter grouping η_B (see equation (13)).

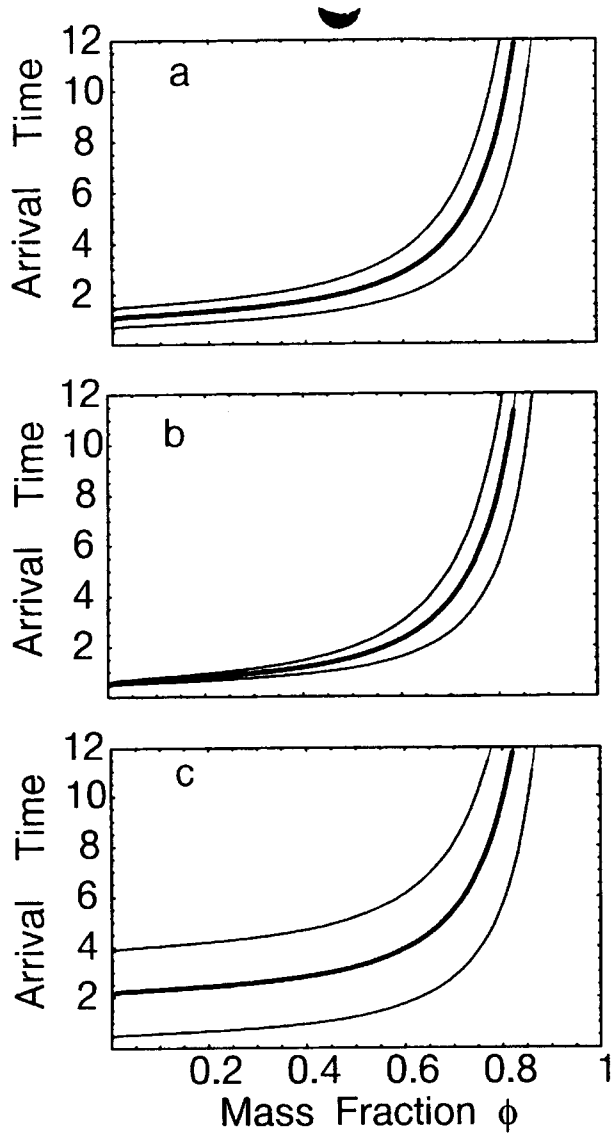

Figure 4. Expected arrival time curve with uncertainty at the outlet of the 50th fracture. Arrival times are normalized by the deterministic arrival time τ_d. The model paramters here are $\eta_B = 1$ and $\sigma^2_{b_1} = \sigma^2_{l_1} = 1$. The length/aperture correlation is different for the three plots. In (a) $\rho = 0$, while $\rho = -3/4$ in (b) and $\rho = 3/4$ in (c).

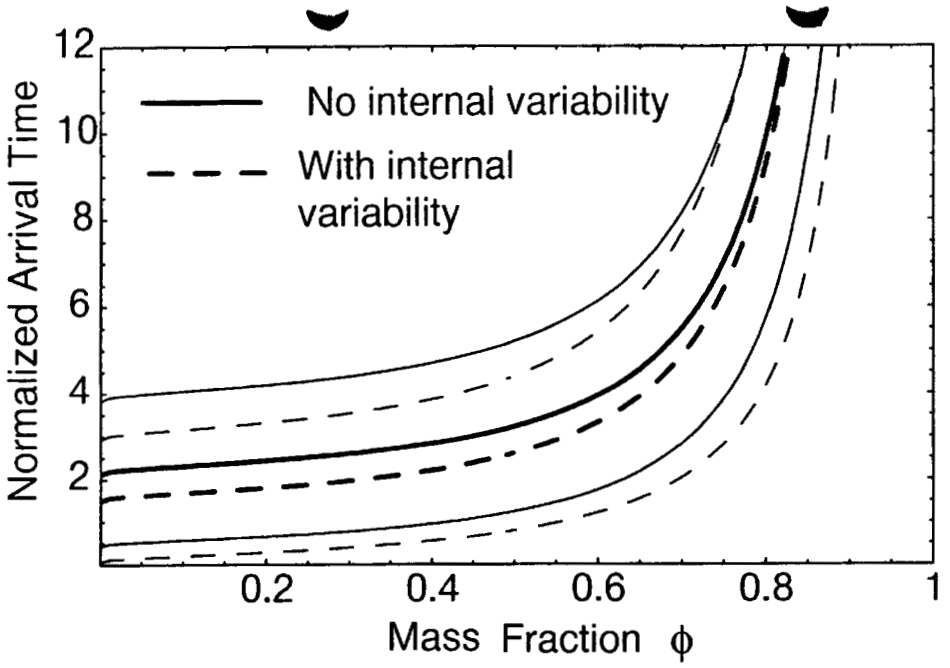

Figure 5. Expected value of the cumulative arrival time curve plus or minus one standard deviation. The solid curves have no internal fracture variability, while the dashed curves have internal variability in addition to fracture-to-fracture variability. Other parameters are the same as in Figure 4c.